Cosmic Masers - from OH to H_0
Proceedings IAU Symposium No. 287, 2012
R.S. Booth, E.M.L. Humphreys & W.H.T. Vlemmings, eds.

doi:10.1017/S1743921312006989

Radio and IR interferometry of SiO maser stars

Markus Wittkowski[1], David A. Boboltz[2], Malcolm D. Gray[3], Elizabeth M. L. Humphreys[1] Iva Karovicova[4], and Michael Scholz[5,6]

[1]ESO, Karl-Schwarzschild-Str. 2, 85748 Garching bei München, Germany

[2]US Naval Observatory, 3450 Massachusetts Avenue, NW, Washington, DC 20392-5420, USA

[3]Jodrell Bank Centre for Astrophysics, Alan Turing Building, University of Manchester, Manchester M13 9PL, UK

[4]Max-Planck-Institut für Astronomie, Königstuhl 17, 69117 Heidelberg, Germany

[5]Zentrum für Astronomie der Universität Heidelberg (ZAH), Institut für Theoretische Astrophysik, Albert-Ueberle-Str. 2, 69120 Heidelberg, Germany

[6]Sydney Institute for Astronomy, School of Physics, University of Sydney, Sydney NSW 2006, Australia

Abstract. Radio and infrared interferometry of SiO maser stars provide complementary information on the atmosphere and circumstellar environment at comparable spatial resolution. Here, we present the latest results on the atmospheric structure and the dust condensation region of AGB stars based on our recent infrared spectro-interferometric observations, which represent the environment of SiO masers. We discuss, as an example, new results from simultaneous VLTI and VLBA observations of the Mira variable AGB star R Cnc, including VLTI near- and mid-infrared interferometry, as well as VLBA observations of the SiO maser emission toward this source. We present preliminary results from a monitoring campaign of high-frequency SiO maser emission toward evolved stars obtained with the APEX telescope, which also serves as a precursor of ALMA images of the SiO emitting region. We speculate that large-scale long-period chaotic motion in the extended molecular atmosphere may be the physical reason for observed deviations from point symmetry of atmospheric molecular layers, and for the observed erratic variability of high-frequency SiO maser emission.

Keywords. masers, radiative transfer, turbulence, techniques: interferometric, stars: AGB and post-AGB, stars: atmospheres, stars: circumstellar matter, stars: fundamental parameters, stars: mass loss, supergiants

1. Introduction

Low to intermediate mass stars, including our Sun, evolve to red giant and subsequently to asymptotic giant branch (AGB) stars. An AGB star is in the final stage of stellar evolution that is driven by nuclear fusion. Mass loss becomes increasingly important during the AGB evolution, both for the stellar evolution, and for the return of material to the interstellar medium. Depending on whether or not carbon has been dredged up from the core into the atmosphere, AGB stars appear to have an oxygen-rich or a carbon-rich chemistry. A canonical model of the mass-loss process has been developed for the case of the carbon-rich chemistry, where atmospheric carbon dust has a sufficiently large opacity to be radiatively accelerated and driven out of the gravitational potential of the star and where it drags along the gas (e.g., Wachter *et al.* 2002, Mattsson *et al.* 2010). For the case of an oxygen-rich chemistry, the details of this process are not understood, and are currently a matter of debate (e.g., Woitke 2006, Höfner 2008). Questions remain also for

the carbon-rich case, such as regarding the recent observational evidence that the oxygen-bearing molecule H_2O is ubiquitous in C-stars (Neufeld *et al.* 2011). Another unsolved problem in stellar physics is the mechanism by which (almost) spherically symmetric stars on the AGB evolve to form axisymmetric planetary nebulae (PNe). Currently, a consensus seems to form that single stars cannot trivially evolve towards non-spherical PNe, by mechanisms such as magnetic fields or rotation, but that a binary companion is required in the majority of the observed PN morphologies (e.g. de Marco 2009).

In order to solve these open questions, it is important to observationally establish the detailed stratification and geometry of the extended atmosphere and the dust formation region, and to compare it to and constrain the different modeling attempts. This includes the following questions: How is the mass-loss process connected to the stellar pulsation? Which is the detailed radial structure of the atmosphere and circumstellar envelope? At which layer do inhomogeneities form? Which are the shaping mechanisms? Which is the effect of inhomogeneities on the further stellar evolution?

2. Synergy of radio and infrared interferometry

Radio and infrared interferometry are both well suited to probe the structure, morphology, and kinematics of the extended atmospheres and circumstellar environment of evolved stars, because of their ability to spatially resolve these regions. In fact, evolved stars have been prime targets for radio and infrared interferometry for decades, because they match well the sensitivity and angular scale of available facilities. Interferometric observations continue to provide new observational results in the field of evolved stars thanks to newly available spectro-interferometry at infrared wavelengths, new radio interferometric facilities, larger samples of well studied targets, and comparisons to newly available theoretical models. Here, radio and infrared interferometry provide complementary information. From the perspective of infrared studies, radio interferometry of SiO, OH, and H_2O maser emission adds information on the morphology and kinematics at different scales from a few stellar radii (SiO maser) to a few hundred stellar radii (OH maser). From the perspective of radio interferometry, infrared interferometry provides information on the environment of the astrophysical masers, including the radiation field, the radii at wavelengths of maser pumping, and constraints on the stratification of the temperature, density, and number densities.

3. Project outline

We have established a project of coordinated interferometric observations of evolved stars at infrared and radio wavelengths. Our goal is to constrain the radial structure and kinematics of the stellar atmosphere and the circumstellar environment to understand better the mass-loss process and its connection to stellar pulsation. We also aim at tracing asymmetric structures from small to large distances in order to constrain shaping processes during the AGB evolution. We use two of the highest resolution interferometers in the world, the Very Large Telescope Interferometer (VLTI) and the Very Long Baseline Array (VLBA) to study AGB stars and their circumstellar envelopes from near-infrared to radio wavelengths. For some sources, we have coordinated near-infrared broad-band photometry obtained at the South African Astronomical Observatory (SAAO) in order to derive effective temperatures. We have started to use the Atacama Pathfinder Experiment (APEX) to investigate the line strengths and variability of high frequency SiO maser emission in preparation of interferometric observation of SiO emitting regions using the ALMA facility.

4. Observations

Our pilot study included coordinated observations of the Mira variable S Orionis including VINCI K-band measurements at the VLTI and SiO maser measurements at the VLBA (Boboltz & Wittkowski 2005). For the Mira variables S Ori, GX Mon, RR Aql and the supergiant AH Sco, we obtained long-term mid-infrared interferometry covering several pulsation cycles using the MIDI instrument at the VLTI coordinated with VLBA SiO (42.9 GHz and 43.1 GHz transitions) observations (partly available in Wittkowski *et al.* 2007, Karovicova *et al.* 2011). For the Mira variables R Cnc and X Hya, we coordinated near-infrared interferometry (VLTI/AMBER), mid-infrared interferometry (VLTI/MIDI), VLBA/SiO maser observations, VLBA/H_2O maser, and near-infrared photometry at the SAAO (first results in Wittkowski *et al.* 2008). Most recently, we obtained measurements of the $v = 1$ and $v = 2$ $J = 7 - 6$ SiO maser transitions toward a sample of evolved stars at several epochs using the APEX telescope.

5. Modeling

We used the P & M model series by Ireland *et al.* (2004a,b) and most recently the CODEX models by Ireland *et al.* (2008, 2011) to describe the dynamic model atmospheres of Mira variable AGB stars. Wittkowski *et al.* (2007) and Karovicova *et al.* (2011) added ad-hoc radiative transfer models to these dynamic model atmosphere series to describe the dust shell. They employed the radiative transfer code `mcsim_mpi` by Ohnaka *et al.* (2007). Gray *et al.* (2009) combined these hydrodynamic atmosphere plus dust shell models with a maser propagation code in order to model the SiO maser emission.

Wittkowski *et al.* (2007) conducted coordinated mid-infrared interferometry using the VLTI/MIDI instrument and observations of SiO maser emission using the VLBA of the Mira variable S Ori. Based on the modeling of the mid-infrared interferometry as outlined above, they showed that the maser emission is located just outside the layer where the molecular layer becomes optically thick at mid-infrared wavelengths ($\sim 10\mu$m), roughly at two photospheric radii, and is close to, and possibly co-located with Al_2O_3 dust. One of the questions that led to the modeling effort by Gray *et al.* (2009) was whether the combined dynamic model atmosphere and dust shell model that was successful to describe the mid-infrared interferometric observations of S Orionis by Wittkowski *et al.* (2007) would also lead to model-predicted locations of SiO maser emission that is consistent with the simultaneous VLBA observations. The input to the maser propagation model included the temperature and density stratification of the successful model of the mid-infrared interferometric data, the radii of the $1.04\,\mu$m continuum layer, and of optically thick layers at IR pumping bands of SiO ($8.13\,\mu$, $4.96\,\mu$, $2.71\,\mu$, and $2.03\,\mu$m), the IR radiation field of the dust model, and the number densities of SiO and its main collision partners (assuming LTE chemistry). Modeled masers indeed formed in rings with radii of 1.8–2.4 photospheric radii, which is consistent with the S Ori VLBA observations, with other observations in the literature, and with earlier such maser propagation models (Gray *et al.* 1995, Humphreys *et al.* 1996). The new models confirm the $v = 1$ ring at larger radii than the $v = 2$ ring. Maser rings, a shock front, and the $8.13\,\mu$m layer appear to be closely related, suggesting that collisional and radiative pumping are closely related spatially and therefore temporally.

6. Infrared and radio interferometry of the Mira variable AGB star R Cnc

R Cancri (R Cnc) is a Mira variable AGB star with a V magnitude between 6.1 and 11.8 and a period of 362 days (Samus *et al.* 2009) at a distance of 280 pc based on the period-luminosity relation by Whitelock *et al.* (2008). We obtained two epochs of observations (23 Dec 2008 to 10 Jan 2009 and 25 Feb 2009 to 3 Mar 2009) that were coordinated between near-infrared spectro-interferometry obtained with VLTI/AMBER, mid-infrared spectro-interferometry obtained with VLTI/MIDI, near-IR $JHKL$ photometry obtained at the SAAO, and VLBA observations of the SiO maser emission and H_2O maser emission. The details of these observations will be available in Wittkowski *et al.* (in preparation). The first epoch of near-infrared spectro-interferometry of R Cnc is available in Wittkowski *et al.* (2011).

6.1. *Near-infrared spectro-interferometry of R Cnc*

Fig. 1 shows the near-infrared squared visibility amplitudes and closure phases of R Cnc obtained with the VLTI/AMBER instrument (from Wittkowski *et al.* 2011). The visibility amplitudes show a characteristic *bumpy* shape that has also been observed in VLTI/AMBER observations of S Ori in Wittkowski *et al.* (2008) and that is interpreted

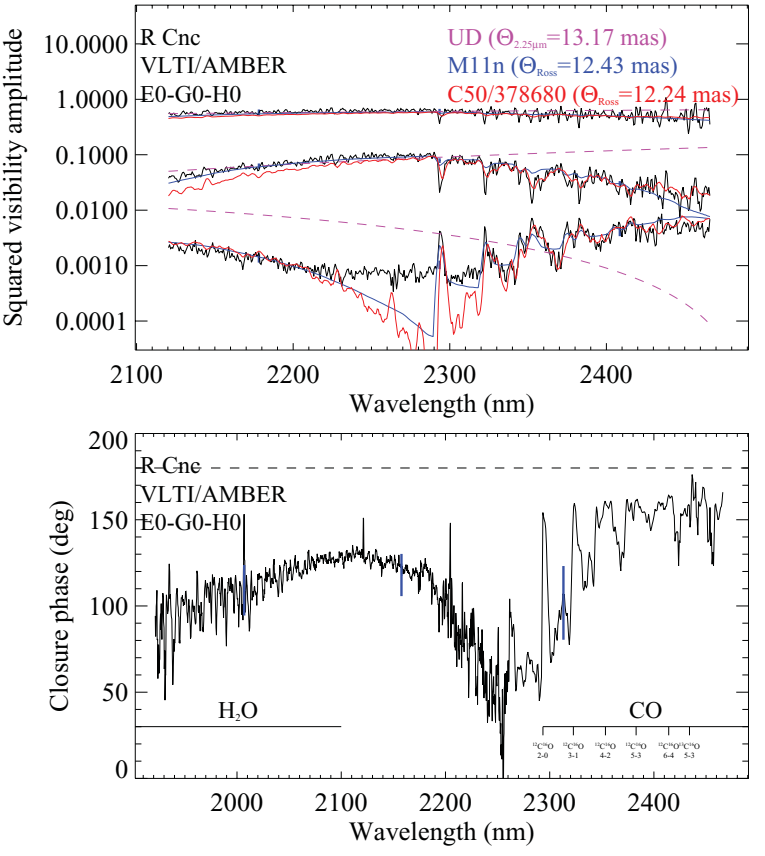

Figure 1. Near-IR squared visibility amplitude (top) and closure phase (bottom) of R Cnc obtained with the VLTI/AMBER instrument from Wittkowski *et al.* (2011). The upper panel also shows predictions by dynamic model atmospheres (M series by Ireland *et al.* 2004a,b, and CODEX series by Ireland *et al.* 2008, 2011).

as being indicative of the presence of molecular layers lying on top of the continuum-forming photosphere and that extend to a few photospheric radii. The visibilities are well consistent with predictions by the latest dynamic model atmosphere series by Ireland *et al.* (2008, 2011) that include such molecular layers. The wavelength-dependent closure phases indicate deviations from point symmetry at all wavelengths and thus a complex non-spherical stratification of the atmosphere. In particular, Wittkowski *et al.* (2008) discuss that the strong closure phase signal in the water vapor and CO bandpasses can be a signature of large-scale inhomogeneities/clumps of the molecular layers. These might be caused by pulsation- and shock-induced chaotic motion in the extended atmosphere as theoretically predicted by Icke *et al.* (1992) and Ireland *et al.* (2008, 2011). We note that these extended atmospheric layers correspond roughly to the radii where SiO maser emission is observed.

6.2. *Mid-infrared spectro-interferometry of R Cnc*

Fig. 2 shows the mid-IR visibility amplitude of R Cnc obtained with VLTI/MIDI from Karovicova (2011). The MIDI data can well be re-produced with a dynamic model atmosphere, which naturally includes molecular layers, and an ad-hoc radiative transfer model of an Al_2O_3 dust shell with an inner radius of ~ 2.2 photospheric radii and an optical depth $\tau_V \sim 1.4$. As in the case of MIDI observations of S Ori (Wittkowski *et al.* 2007), R Cnc does not show an indication of an additional silicate dust shell. The inner radius of the Al_2O_3 dust shell is located at a radius that is close to the radius where SiO maser emission is observed. Oher sources that have been studied by Karovicova (2011) show either Al_2O_3 dust, silicate dust, or both dust species. Karovicova (2011) discussed an indication that the dust content of stars with low mass-loss rates is dominated by Al_2O_3, while the dust content of stars with higher mass-loss rates predominantly exhibit significant amounts of silicates, as suggested by Little-Marenin & Little (1990) and Blommaert *et al.* (2006).

6.3. *VLBA observation of the SiO maser emission toward R Cnc*

Fig. 3 shows our two epochs of VLBA images of the $J = 1 - 0$, $v = 2$ (42.8 GHz) and $J = 1 - 0$, $v = 1$ (43.1 GHz) SiO maser emission toward R Cnc. The two epochs are separated by about 7 weeks. The two transitions were registered to each other by transferring the calibration from one transition to the other. Consistently with earlier

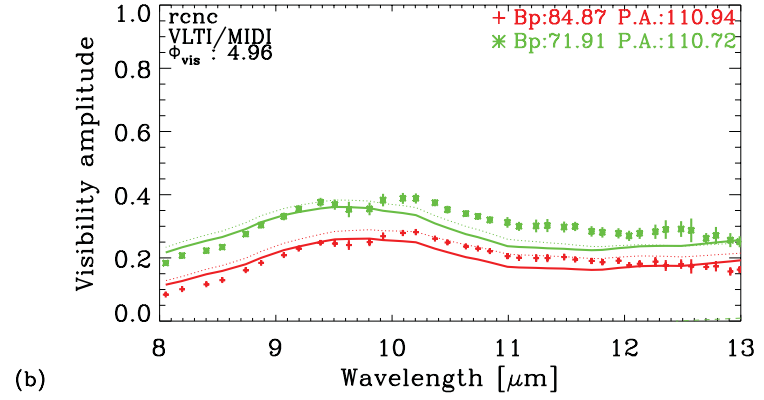

Figure 2. Mid-IR visibility amplitude of R Cnc obtained with VLTI/MIDI from Karovicova (2011). Also shown is a model of a dynamic model atmosphere combined with a radiative transfer model of the dust shell (see text).

observations, the $v = 1$ transition is located at larger radii than the $v = 2$ transition, but with more overlap at epoch 1 and a clearer separation at epoch 2. The morphology is more ring-like at epoch 2 compared to epoch 1.

7. Monitoring of high-frequency SiO maser emission toward evolved stars

Observations of high-frequency SiO maser emission has been shown to be more variable than centimeter SiO maser emission, indicating that high-frequency maser emission depends more strongly on the environmental conditions of the masers, and that

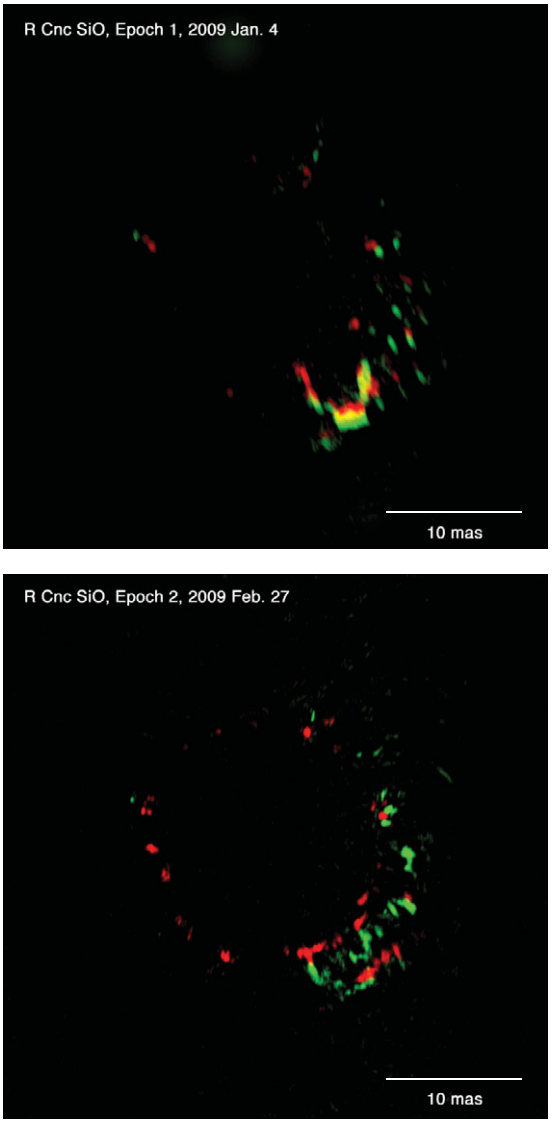

Figure 3. VLBA observations of the SiO emission toward R Cnc at two epochs (top: 4 Jan 2009, bottom: 27 Feb 2009). The red maps denotes the $J = 1-0$, $v = 2$ transition and the green maps the $J = 1 - 0$, $v = 1$ transition.

thus their observations may provide stronger observational constraints (Gray *et al.* 1995, Humphreys *et al.* 1997, Gray *et al.* 1999).

Following these studies, we have established a monitoring of high-frequency $J = 7-6$, $v = 1, 2, 3$ SiO maser emission toward a sample of AGB stars in order to compare their variability to the predictions by Gray *et al.* (2009). This represents also an important precursor of ALMA imaging studies of the SiO emitting regions of evolved stars.

Our observational results suggest that the variability is erratic. It does not appear to be correlated with the stellar phase and is also not consistent among the different sources of our sample. For, example, o Cet showed $v = 1$ emission at all phases between stellar minimum and post-maximum with increasing intensity, and $v = 2$ emission only at post-maximum (phase 1.1) with lower intensity compared to $v = 1$ emission at this phase (Fig. 4). To the contrary, R Hya, for instance, shows $v = 1$ emission only at post-maximum (1.1) but not between minimum and maximum, but $v = 2$ emission at all phases between 0.5 and 1.1 and at phase 1.1 with higher intensity compared to $v = 1$. R Leo showed both $v = 1$ and $v = 2$ emission at phases between 0.5 and 0.8 with alternating ratio between the strength of the $v = 1$ and $v = 2$ emission.

We hypothesize that large-scale (a few cells across the stellar surface) long-period (times scales corresponding to a few pulsation cycles) chaotic motion in the extended atmosphere, induced by the interaction of pulsation and shock fronts with the extended atmosphere, and a possibly related erratic variability of the SiO abundance, may be the reason for our observed erratic maser variability.

8. Summary

Near-infrared interferometry of oxygen-rich evolved stars indicates a complex atmosphere including extended atmospheric molecular layers (in the IR most importantly H_2O, CO, SiO), which is consistent with predictions by the latest dynamic model atmospheres. Near-IR closure phases indicate a complex non-spherical stratification of the atmosphere, indicating asymmetric/clumpy molecular layers. These are possibly caused by chaotic motion in the extended atmosphere, which may be triggered by the pulsation in the stellar interior. Mid-infrared interferometry constrains dust shell parameters including Al_2O_3 dust with inner radii of typically two photospheric radii and silicate dust with inner radii of typically four photospheric radii. SiO masers lie in the extended atmosphere as seen by infrared interferometry. They are located just outside the radius where the molecular layer becomes optically thick at mid-IR wavelengths. There are located

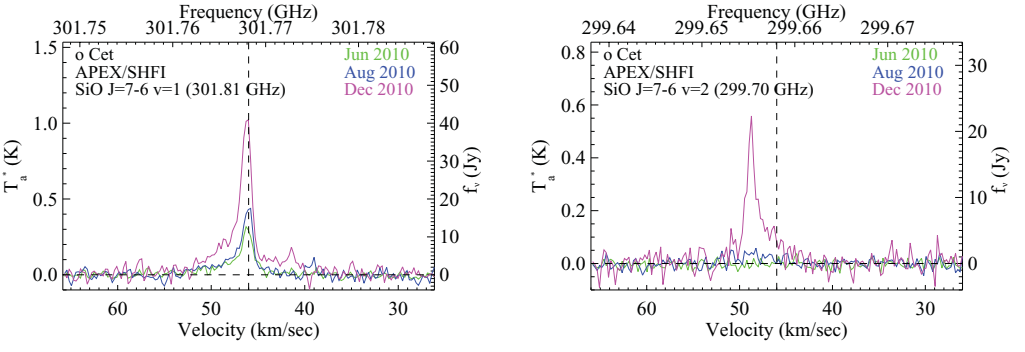

Figure 4. APEX observations of the $J = 7-6$, $v = 1$ (left) and $v = 2$ (right) SiO maser emission of o Cet at three epochs in June 2010 (phase 0.5), August 2010 (phase 0.7), and December 2010 (phase 1.1).

close-to, possibly co-located, with Al_2O_3 dust. Their location is consistent with dynamic model atmospheres combined with a maser propagation code. They are also located at the distances where the near-IR interferometry indicates a clumpy morphology. APEX detects a strong and erratic variability of high-frequency maser emission. We speculate that the erratic variability may be connected to chaotic motion in the extended atmosphere, i.e. to the same mechanism that may lead to the observed clumpyness of extended atmospheric molecular layers.

Acknowledgements

This article is based on a project of coordinated VLTI and VLBA observations of evolved stars to which several people have contributed during the last years in addition to the authors of this article, including Carlos de Breuck, Thomas Driebe, Eric Fossat, Michael Ireland, Keiichi Ohnaka, Anita Richards, Francois van Wyk, Patricia Whitelock, Peter Wood, and Albert Zijlstra.

References

Blommaert, J. A. D. L., Groenewegen, M. A. T., Okumura, K., *et al.* 2006, *A&A*, 460, 555
Boboltz, D. A. & Wittkowski, M. 2005, *ApJ*, 618, 953
De Marco, O. 2009, *PASP*, 121, 316
Gray, M. D., Ivison R., Yates J., Humphreys E., Hall P., & Field D., 1995, *MNRAS*, 277, L67
Gray, M. D., Humphreys, E. M. L., & Yates, J. A. 1999, *MNRAS*, 304, 906
Gray, M. D., Wittkowski, M., Scholz, M., *et al.* 2009, *MNRAS*, 394, 51
Höfner, S. 2008, *A&A*, 491, L1
Humphreys E. M. L., Gray M., Yates J., Field D., Bowen G., & Diamond P., 1996, *MNRAS*, 282, 1359
Humphreys, E. M. L., Gray, M. D., Yates, J. A., & Field, D. 1997, *MNRAS*, 287, 663
Icke, V., Frank, A., & Heske, A. 1992, *A&A*, 258, 341
Ireland, M. J., Scholz, M., & Wood, P. R. 2004a, *MNRAS*, 352, 318
Ireland, M. J. Scholz, M. Tuthill, P. G., & Wood, P. R. 2004b, *MNRAS*, 355, 444
Ireland, M. J., Scholz, M., & Wood, P. R. 2008, *MNRAS*, 391, 1994
Ireland, M. J., Scholz, M., & Wood, P. R. 2011, *MNRAS*, 418, 114
Karovicova, I., Wittkowski, M., Boboltz, D. A., *et al.* 2011, *A&A*, 532, A134
Karovicova, I., 2011, *PhD thesis*, University of Nice
Little-Marenin, I. R. & Little, S. J. 1990, *AJ*, 99, 1173
Mattsson, L., Wahlin, L., & Höfner, S. 2010, *A&A*, 509, A14
Neufeld, D. A., González-Alfonso, E., & Melnick, G. J., *et al.* 2011, *ApJL*, 727, L28
Ohnaka, K., Driebe, T., Weigelt, G., & Wittkowski, M. 2007, *A&A*, 466, 1099
Samus, N. N., Durlevich, O. V., *et al.* 2009, *VizieR Online Data Catalog*, 2025
Wachter, A., Schröder, K.-P., Winters, J., Arndt, T., & Sedlmayr, E. 2002, *A&A*, 384, 452
Whitelock, P., Feast, M. W., & van Leeuwen, F. 2009, *MNRAS*, 386, 313
Wittkowski, M., Boboltz, D. A., Ohnaka, K., Driebe, T., & Scholz, M. 2007, *A&A*, 470, 191
Wittkowski, M., Boboltz, D. A., Driebe, T., *et al.* 2008, *A&A*, 479, L21
Wittkowski, M., Boboltz, D. A., Ireland, M., *et al.* 2011, *A&A*, 532, L7
Woitke, P. 2006, *A&A*, 452, 537